Journal of Catalysis **188,** 24–31 (1999)
Article ID jcat.1999.2648, available online at http://www.idealibrary.com on IDEAL®

Catalytic Reactions of NO over 0–7 mol% Ba/MgO Catalysts

I. The Direct Decomposition of NO

Shuibo Xie, Michael P. Rosynek, and Jack H. Lunsford[1]

Department of Chemistry, Texas A&M University, College Station, Texas 77843

Received January 12, 1999; revised July 20, 1999; accepted July 26, 1999

A series of catalysts composed of barium oxide supported on magnesium oxide with Ba loadings up to 7 mol% has been studied for NO and N_2O decomposition. Nitrous oxide is an intermediate in the decomposition of nitric oxide; however, the rate of N_2O decomposition is much greater than that of NO decomposition so that the selectivity for N_2 formation approaches 100% at $T > 700^\circ C$. Over 4 mol% Ba/MgO catalyst, the rate of N_2 formation at 800°C was 0.22 $\mu mol\, g^{-1} s^{-1}$ for a gas stream containing 1% NO in He. When the inhibiting effect of O_2 is properly accounted for, the reaction order with respect to NO is two. This order is consistent with a mechanism in which gas-phase NO reacts with a surface NO_x species that is probably present in an ionic form, considering the temperatures at which the reaction occurs. ***In situ*** **Raman spectroscopy has demonstrated the presence of nitrate and nitrite ions on the surface, but the exact nature of the surface intermediate is not known.** © 1999 Academic Press

Key Words: **nitric oxide; nitrous oxide; barium oxide; decomposition.**

1. INTRODUCTION

Although considerable progress has been made in the selective catalytic reduction (SCR) of NO, the direct decomposition of this thermodynamically unstable molecule remains as a challenging problem in heterogeneous catalysis. Since the discovery by Iwamoto and co-workers (1) in the 1980s that Cu–ZSM-5 catalysts are active for both the decomposition and the SCR of NO, considerable effort has been devoted to this and other zeolite-based catalysts. But even with Cu–ZSM-5, the activity is insufficient for practical utilization, and the catalyst is vulnerable to deactivation by water (2, 3). Recently, Chang and McCarty (4) have reported that a Co–ZSM-5 zeolite that contains Co in the framework has a considerably larger maximum activity for NO decomposition than does a Cu–ZSM-5 zeolite.

Many metal oxides have moderate activity for NO decomposition, including Ag-promoted cobalt oxide (5), oxygen-deficient Sr–Fe oxides (6), and certain perovskite-type compounds such as La–Sr–Co oxides, YBaCuO, and LaSrCuO (7–9). In the early work carried out by Winter in the 1970s (10), more than 40 metal oxides were tested for NO decomposition activity. Recently, Vannice and co-workers (11–14) examined several alkaline earth and rare earth oxides (e.g., Li/MgO and Sr/La_2O_3) and found that they also are active for NO decomposition. Oxygen defects on the surface are suggested as the active centers for NO decomposition (10), although the nature of these oxygen defects is still not clear. Oxygen strongly inhibits the NO decomposition, and it has been suggested that O_2 either decreases the number of defects or inhibits the desorption of oxygen from the catalyst.

We have shown that barium oxide supported on magnesium oxide (Ba/MgO) with barium loadings ≥11 mol% is an unusual catalyst for NO decomposition in that the activity sharply decreases, in a reversible manner, when the reaction temperature exceeds a certain value (15). The fall-off temperature is typically in the range 630 to 700°C, depending on the concentration of NO and, consequently, the O_2 partial pressure. Comparison of catalytic data with Raman spectroscopy results indiates that a barium-nitro species is an intermediate in the catalytic cycle below the fall-off temperature.

The present study was undertaken to determine the catalytic properties of Ba/MgO catalysts at barium loadings ≤7 mol%, which do not exhibit the unusual maximum in activity during NO decomposition. As will be shown, the behaviors of the Ba/MgO catalysts with low loadings of barium are comparable to those of the Sr/La_2O_3 catalyst reported by Vannice and co-workers (14), rather than to the Ba/MgO catalysts with high loadings. At the lower Ba loading levels, there is no spectroscopic evidence for nitro species on the Ba/MgO catalyst; rather, it appears that another ionic NO_x species may be involved in NO decomposition. The primary focus of this study was on the decomposition of NO; however, the formation and decomposition of N_2O was of interest as an elementary step in the overall reaction. Moreover, N_2O itself is also a pollutant that must be controlled. The role of oxygen in inhibiting NO

---

[1] To whom correspondence should be addressed. E-mail: Lunsford @mail.chem.tamu.edu.

0021-9517/99 $30.00

decomposition is discussed in Part I, and the role of CO_2 is briefly described in Part II (16). The effects of other gases such as SO_2 and H_2O were not investigated.

2. EXPERIMENTAL

The BaO/MgO catalyst was prepared by adding a $Ba(NO_3)_2$ (Baker) solution containing the required amount of Ba to a slurry consisting of 5.0 g MgO (Fisher, light) and 30 ml deionized water. The $Ba(NO_3)_2$ solution was added dropwise at 25°C while the MgO slurry was vigorously stirred. The slurry was stirred overnight and the water was evaporated at 100°C. The catalyst was then dried in air at 700°C for 2 h, pressed under 1,360 kg cm^{-2}, crushed, and sieved to 20–40 mesh size. The surface areas of the catalysts were obtained using the BET method with a Quanta Chrome system. Nitrogen gas was used as the adsorbate, while helium was used as the carrier gas. The surface areas of Ba/MgO catalysts, which were unchanged during NO decomposition, are reported in Table 1.

Catalytic results were obtained using a 4-mm i.d. fused-quartz, single-pass, down-flow reactor at atmospheric pressure. Typically, 100 mg or 200 mg catalyst was contained between two layers of quartz wool, and the space upstream from the catalyst bed was filled with fused-quartz chips. The catalysts were pretreated for 1 h (or longer as needed to decompose the carbonate formed during catalyst preparation) at 800°C in a 10% mixture of O_2 in He at a flow rate of 20 ml min^{-1} and cooled to 25°C in this gas mixture. Then the catalysts were heated to the reaction temperature in a mixture of flowing reagent gas. Reaction mixtures were obtained by adding 4% NO/He (or 1% N_2O/He) to pure He to obtain the desired gas compositions. The total flow rate was 40 ml min^{-1} (760 Torr, 25°C). Before the data were obtained, reactions were maintained for a period of 50 min at each temperature to ensure steady-state conditions.

Analyses of the gases after reaction were performed with an HP5890 gas chromatograph, equipped with a 9-m HayeSep DB column (Alltech). The equilibrium reaction $NO + 1/2\ O_2 \rightleftarrows NO_2$ is favored at low temperatures, and the formation of NO_2 is expected to occur in the cool region downstream from the reactor. Therefore, no attempt was made to quantify NO_2 or O_2. The NO conversion was obtained from the relationship $2([N_2]+[N_2O])/[NO]_0$, where $[NO]_0$ is the concentration of nitric oxide in the feed gas mixture; the N_2 selectivity was obtained from the relationship $[N_2]/([N_2]+[N_2O])$.

Rate laws and activation energies were based on NO conversions that did not exceed 20%. In a few cases the rate of reaction was obtained at a larger conversion level by means of an integrated rate equation, assuming a power rate law that was 1.5 order with respect to NO (see below).

Raman data were obtained using a Holoprobe Raman spectrometer (Kaiser Optical) system that was equipped with an Nd:YAG laser. The frequency-doubled laser (532 nm) was operated at 25 mW. A more complete description of the system, including the flow-through cell, has been published previously (17).

3. RESULTS

3.1. *The Decomposition of NO and N_2O over Ba/MgO Catalysts*

Nitric oxide direct decomposition over a series of Ba/MgO catalysts with different Ba loadings was studied in the temperature range from 500 to 850°C, and the results are shown in Fig. 1. The reagent gas was a 1% NO/He mixture with a flow rate of 40 ml/min (760 Torr, 25°C). For the catalysts with Ba loadings up to 7 mol%, the specific N_2 formation rates increased in a monotonic manner up to 850°C. While pure MgO was essentially inactive for NO

TABLE 1

BET Surface Areas of Ba/MgO Catalysts, Reaction Rates, and Activation Energies for 1% NO Decomposition over Ba/MgO Catalysts

Catalysts	Surface area ($m^2\ g^{-1}$)	Reaction rates at 700°C (μmol $g^{-1}\ s^{-1}$)	Reaction rates at 700°C (μmol $m^{-2}\ s^{-1}$)	Activation energy (kcal/mol^{-1})
MgO	38.3	4.4×10^{-3}	1.2×10^{-4}	—
0.5 mol% Ba/MgO	36.6	5.0×10^{-3}	1.4×10^{-4}	—
1 mol% Ba/MgO	35.1	1.2×10^{-2}	3.5×10^{-4}	36.2
4 mol% Ba/MgO	23.1	6.8×10^{-2}	3.0×10^{-3}	39.9
7 mol% Ba/MgO	6.0	2.2×10^{-2}	3.6×10^{-3}	24.2
14 mol% Ba/MgO[a]	3.2	2.5×10^{-1}	7.8×10^{-2}	—
4 wt% Sr/La_2O_3[b]	1.7	3.6×10^{-2}	2.1×10^{-2}	28
1 wt% Sr/La_2O_3[c]	5.4	2.9×10^{-2}	5.4×10^{-3}	38.4

[a] From Ref. (15); rates reported at 630°C, which was the temperature corresponding to the maximum in activity.

[b] From Ref. (14); normalized to 1% NO.

[c] From Ref. (23).

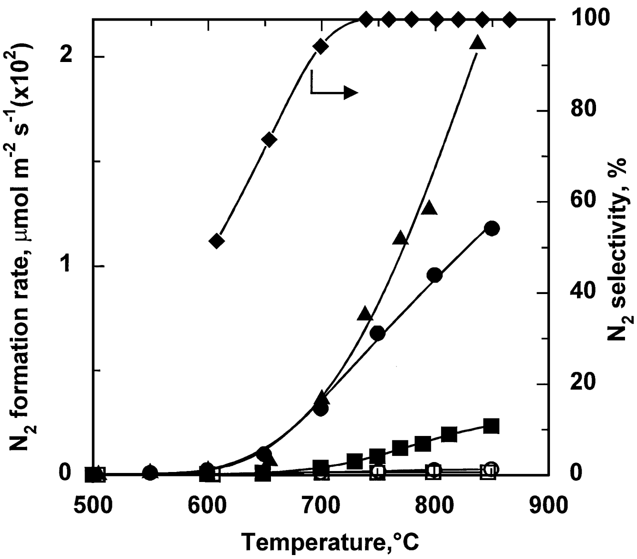

FIG. 1. Nitrogen formation rates during 1% NO decomposition over Ba/MgO catalysts with different Ba loadings: (□) MgO, (○) 0.5 mol% Ba/MgO, (■) 1 mol% Ba/MgO, (●) 4 mol% Ba/MgO, (▲) 7 mol% Ba/MgO, (◆) N_2 selectivity over 4 mol% Ba/MgO.

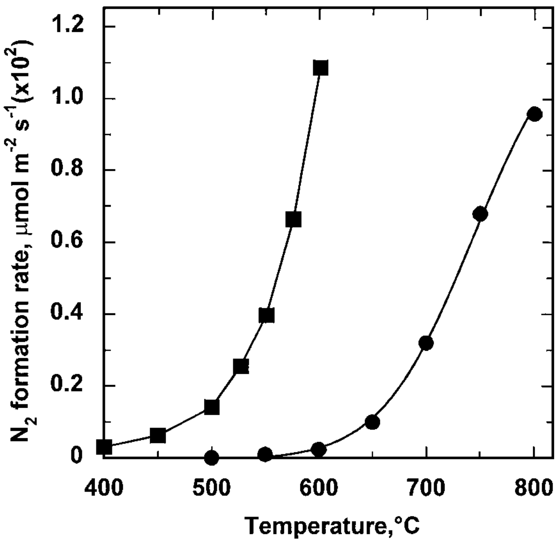

FIG. 2. Nitrogen formation rates during NO and N_2O decomposition over a 4 mol% Ba/MgO catalyst: (●) 1% NO, (■) 0.5% N_2O.

decomposition, the specific rates increased upon the addition of BaO, and the 7 mol% Ba/MgO catalyst appeared to be the most active. However, on a per gram basis, the 4 mol% Ba/MgO catalyst was the most active, as shown in Table 1, among the catalysts with Ba loadings up to 7 mol%. At 800°C, the conversion over 200 mg of the 4 mol% Ba/MgO catalyst was ca. 30%, and the rate, on a per gram basis, was 0.22 μmol g^{-1} s^{-1}. It is apparent from the results in Fig. 1 that the rate over this catalyst did not increase exponentially with respect to temperature in the range 750–850°C, which is a result of the poisoning effect of the product O_2 (see below). On a per m^2 basis, the 4- and 7-mol% samples had comparable rates, which were about an order of magnitude larger than that of the 1 mol% sample.

Besides N_2 and O_2, N_2O was also observed as a product of NO decomposition. As shown in Fig. 1, the N_2 selectivity in NO decomposition products over a 4 mol% Ba/MgO catalyst increased with increasing temperature. While equal amounts of N_2 and N_2O were formed at 600°C, no N_2O was observed in the products when the reaction temperature was above 700°C. Nitrous oxide has been proposed as a reaction intermediate for nitrogen formation during NO decomposition (18); therefore, the role of N_2O in NO decomposition over the Ba/MgO catalyst was also studied. In Fig. 2, the rates of decomposition of 0.5% N_2O and 1% NO over a 4% Ba/MgO catalyst are compared. The 4 mol% Ba/MgO catalyst was found to be very active for N_2O decomposition; the conversion of N_2O reached 100% over 200 mg catalyst at temperatures greater than 700°C. The activation energy for N_2O decomposition was 31.8 kcal mol^{-1}. The rate of N_2O decomposition is much larger than that of NO decomposition; e.g., the N_2 formation rate from the decomposition of 0.5% N_2O was 260 times that of 1% NO decomposition at 600°C. It is likely that N_2 is formed during NO decomposition via the decomposition of N_2O over a 4 mol% Ba/MgO catalyst. The role of N_2O as a reaction intermediate in NO decomposition was confirmed by the results of a separate experiment in which the space velocity of the 4% NO reagent gas was varied. The concentrations of N_2O and N_2 in the downstream products as a function of contact time are given in Fig. 3. As the contact time increased, the N_2 concentration increased continuously, while the N_2O concentration exhibited a maximum at a

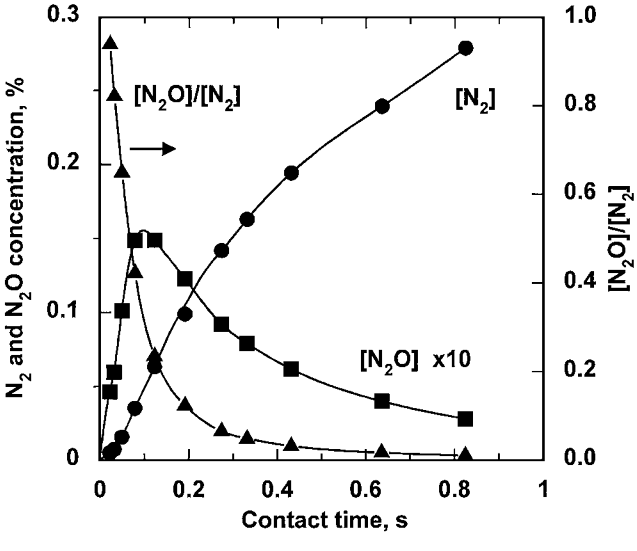

FIG. 3. Product distribution during 4% NO decomposition as a function of contact time. Catalyst, 200 mg 4 mol% Ba/MgO; $T = 680$°C.

contact time of about 0.1 s, and the $[N_2O]/[N_2]$ ratio decreased continuously. The concentration profile of downstream products during NO decomposition and the inflection in N_2 concentration at short contact times (<0.1 s) is typical for consecutive reactions, indicating that N_2O is an intermediate in the decomposition of NO; i.e., the reaction pathway for nitrogen formation can be expressed by $NO \rightarrow N_2O \rightarrow N_2$.

3.2. The Effect of Oxygen on the Decomposition of NO and N_2O

Oxygen has an inhibiting effect on the activity of Ba/MgO catalysts for the decomposition of NO and, to a lesser extent, the decomposition of N_2O. A negative reaction order with respect to oxygen has been reported for NO decomposition over metal oxides and supported Pt catalysts (19). To investigate the effect of oxygen on the rate of NO decomposition over the 4 mol% Ba/MgO catalyst, 0.5% O_2 was introduced into the reagent gas containing 1% NO. In one set of experiments, NO and O_2 were premixed at room temperature before they were placed in the reactor, and in another set of experiments, NO and O_2 were mixed in the hot zone of the reactor by introducing O_2 ca. 1 cm above the catalyst bed via a small fused-quartz tube. In the latter case, NO_2 formation via the reaction of NO and O_2 was avoided. Nitrogen dioxide is not thermodynamically stable at the high temperatures employed in these catalytic reactions.

It is evident from Fig. 4 that the nitrogen formation rate from 1% NO decomposition is less in the presence of 0.5% O_2 than in the absence of added O_2 over the temperature region examined, and the oxygen inhibiting effect for NO decomposition appears to be more significant at lower reaction temperatures. The addition of 0.5% O_2 reduced the N_2 formation rate about 80% (from 2.3×10^{-4} to 0.46×10^{-4} μmol m^{-2} s^{-1}) at 600°C but only 47% (from 9.6×10^{-3} to 5.1×10^{-3} μmol m^{-2} s^{-1}) at 800°C. The inhibiting effect of O_2 on NO decomposition was independent of whether NO and O_2 were premixed outside the reactor at room temperature or mixed inside the reactor at high temperatures. In addition, the rates of 1% NO_2 decomposition over 4 mol% Ba/MgO are lower than those of 1% NO + 0.5% O_2 at $T \geq 650$°C (Fig. 4). These results suggest (i) that NO_2 was not formed in a significant amount prior to the reagents entering the heated zone and (ii) when NO_2 was purposely introduced, it did not rapidly dissociate to NO and O_2 over the catalyst. The important point is that NO_2 was not a factor in determining the effect of O_2 on NO decomposition. A slight inhibiting effect of O_2 on the rate of N_2O decomposition was also observed, as shown in Fig. 5; however, the effect was much less than that during NO decomposition. Only at temperatures less than 600°C was the *percentage* decrease appreciable (45% at 503°C and 11% at 601°C).

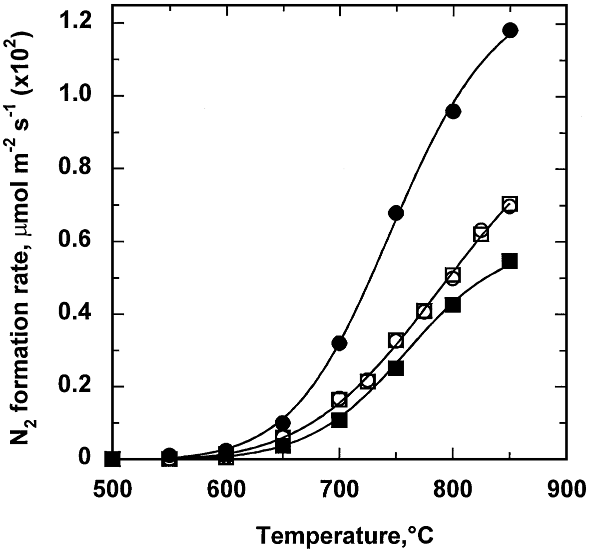

FIG. 4. Comparison of N_2 formation rates from different reagent gases over a 4 mol% Ba/MgO catalyst. Catalyst weight, 200 mg. (●) 1% NO, (○) 1% NO + 0.5% O_2 (premixed outside reactor), (□) 1% NO + 0.5% O_2 (mixed inside the reactor hot zone), (■) 1% NO_2.

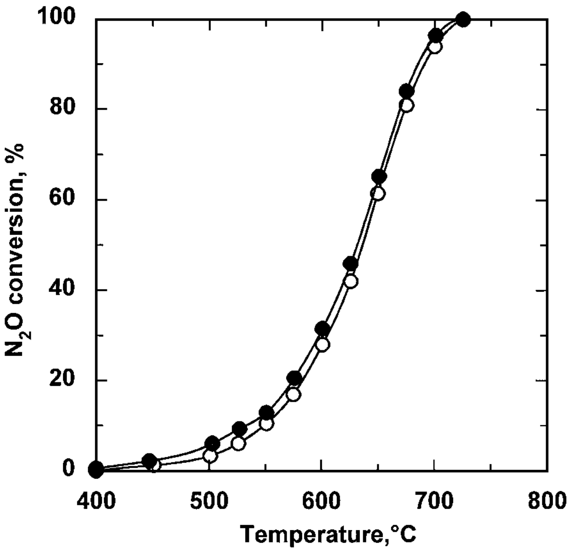

FIG. 5. The effect of addition of 0.5% O_2 on N_2O decomposition over a 4 mol% Ba/MgO catalyst: (●) 0.5% N_2O, (○) 0.5% N_2O + 0.5% O_2.

3.3. Determination of Kinetic Parameters for NO Decomposition

The activation energies for NO decomposition over these Ba/MgO catalysts and a 1 wt% Sr/La_2O_3 catalyst were measured in the temperature region 600–800°C, and the results are shown in Table 1. The activation energies are similar for the Ba/MgO catalysts and the Sr/La_2O_3 catalyst, with values between 36 and 40 kcal/mol, except for the 7 mol% Ba/MgO catalyst, which exhibited an unusually low value of 24.2 kcal/mol. The value observed previously (15) for the 14 mol% Ba/MgO catalyst, above the fall-off temperature, was 13 kcal mol^{-1}. Thus, at the higher Ba loadings there is a significant decrease in activation energy.

Regarding the reaction order with respect to NO, both first-order and second-order have been reported during the direct decomposition of NO over metal oxides (10, 19, 20). The method used to determine the reaction order was to monitor the N_2 formation rates as a function of NO concentration in the feed gas. However, the situation is complicated by the O_2 poisoning effect, which was neglected in previous studies of the reaction order. The amount of O_2 generated from NO decomposition is different for different NO concentrations in the feed gas; more O_2 is formed when the NO concentration in the feed gas increases, if one assumes that the reaction order with respect to NO is positive. Therefore, the activity decrease caused by the oxygen in the products would not be the same for all NO concentrations. The dependence of N_2 formation rates as a function of the concentration of O_2 added is clearly shown in Fig. 6. The addition of a small amount of O_2 caused the activity to decrease significantly, but the inhibiting effect of O_2 leveled off at high O_2 concentrations. Since the inhibiting effect of O_2 is more significant at higher NO concentrations, due to the higher concentration of O_2 produced from NO decomposition, it is expected that the apparent reaction order with respect to NO, determined without taking account of this O_2 effect, would be less than the actual value. In this study, 2% O_2, which is in excess of the amount generated from NO decomposition, was added to the feed gas in order to create conditions such that the reaction was pseudo zero order in O_2. To avoid complications due to the formation of NO_2, the O_2 was introduced in the heated region of the reactor, about 1 cm above the catalyst bed.

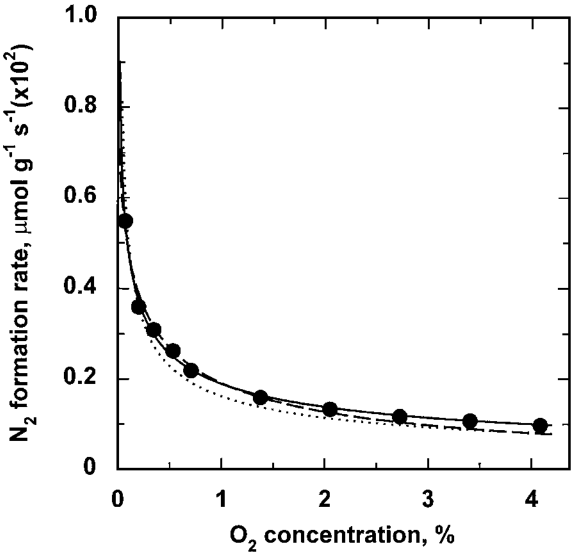

FIG. 6. The effect of oxygen on the N_2 formation rate over a 4 mol% Ba/MgO catalyst. Reagent gas was 1% NO with different O_2 concentrations. $T = 750°C$. (●) Experimental data, (---) fitted with Eq. [5], (···) fitted with Eq. [11], (—) fitted with Eq. [17].

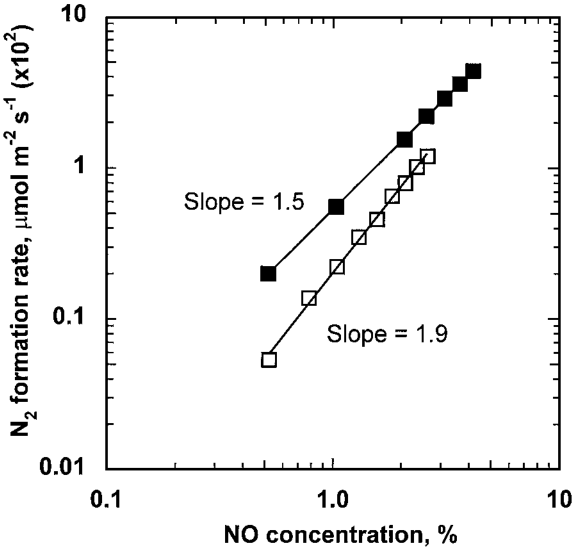

FIG. 7. Nitrogen formation rate as a function of NO concentration over a 4 mol% Ba/MgO catalyst. $T = 850°C$. (■) No O_2 added, total flow rate = 120 ml/min; (□) in the presence of 2% O_2, total flow rate = 40 ml/min.

The N_2 formation rate as a function of NO concentration over a 4 mol% Ba/MgO catalyst at 850°C in the absence and presence of added O_2 is shown in Fig. 7. In both cases, the NO conversions were kept at less than 20%; thus, the reactions were carried out under nearly differential conditions. In the absence of added O_2, the total flow rate was increased from 40 to 120 ml min^{-1} to maintain an NO conversion <20%, and the apparent reaction order with respect to NO was 1.5. The reaction order determined in the presence of 2% O_2 was 1.9, which is believed to be closer to the actual value. Although this value is slightly less than 2, it is quite reasonable to conclude that NO decomposition over Ba/MgO catalysts is a second-order reaction, if one takes account of the fact that the reaction rate is still suppressed at higher O_2 concentrations, even in the presence of 2% O_2. For the lowest and highest NO concentrations employed in determining the NO reaction order in the presence of 2% O_2, the NO conversion was 3.5 and 15.7%, respectively; correspondingly, the actual O_2 concentration in the exit gas was 2.02 and 2.18%, respectively.

3.4. *Surface Intermediates*

In order to better understand the surface chemistry of Ba/MgO catalysts during the NO decomposition, *in situ* Raman spectroscopy was used to monitor the change of a 4 mol% Ba/MgO catalyst under reaction conditions. The

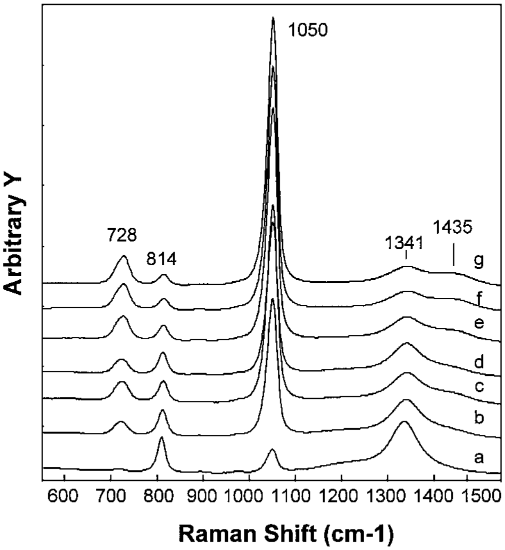

FIG. 8. Raman spectra recorded at 600°C in 1% NO with different O_2 concentrations: (a) 1% NO, (b) 1% NO + 0.25% O_2, (c) 1% NO + 0.5% O_2, (d) 1% NO + 1% O_2, (e) 1% NO + 2.5% O_2, (f) 1% NO + 5% O_2, (g) 1% NO + 7% O_2.

Raman spectra were first recorded at 600°C. Reagent gases containing 1% NO and O_2 concentrations between 0 and 7% flowed through the catalyst bed. The spectra shown in Fig. 8 are characterized by bands at 1050 and 728 cm^{-1}, which are due to nitrate ions, and bands at 1341 and 814 cm^{-1}, which are due to nitrite ions (17). The weak band at 1435 cm^{-1} may be an overtone of the band at 728 cm^{-1}. The amplitudes of both sets of bands progressively decreased with increasing temperature. As the oxygen concentration was increased in the feed gas, the concentration of the nitrate species increased, which is indicated by an increase in the amplitude of the Raman bands at 1050 and 728 cm^{-1}. Meanwhile, the amplitude of the Raman bands at 1341 and 814 cm^{-1} decreased. The effect was reversed by switching off the O_2. If the Raman results in Fig. 8 are compared to the catalytic results in Fig. 7, one may at least exclude the role of the nitrate species as a reaction intermediate. On the other hand, the Raman results suggest that the nitrite species may serve as an intermediate during NO decomposition, through reaction with a gas phase or a weakly adsorbed NO molecule to form N_2O. The role of nitrite ions in NO decomposition, however, is not as straightforward as indicated by the results of Fig. 8 because at 650°C the amplitude of both nitrate and nitrite bands increased with the addition of O_2 (spectra not shown). As noted previously (15), the barium-nitro species, which is believed to be the principal intermediate in NO decomposition over a 14 mol% Ba/MgO catalyst, is not present on the 4 mol% Ba/MgO sample in significant amounts, as indicated by the absence of a Raman band at 1322 cm^{-1} and bands at 400, 244, and 143 cm^{-1} (this region of the spectra not shown).

4. DISCUSSION

The effect of loading on catalytic activity (Fig. 1 and Table 1) is not fully understood; however, based on Raman and X-ray diffraction (XRD) evidence, as well as other catalytic studies, it is evident that significant changes occur over the loading range 2–4 mol% Ba (21, 22). The most dramatic of these was a sharp increase in the Raman band due to crystalline BaO_2 when the loading was increased from 2 to 4 mol% (21). These samples had been pretreated in O_2 for 4 h at 800°C. In addition to the Raman results, lines due to the BaO_2 began to appear in the diffraction pattern when the loading reached 4 mol% Ba. But ion scattering spectroscopy (ISS) indicated that, at least for the 2 mol% Ba/MgO sample, Mg^{2+} ions were still exposed on the surface (22). On the catalyst of Ref. (22), 2 mol% Ba/MgO would have significantly exceeded the monolayer equivalent since the surface area of this sample was only 8.8 $m^2\ g^{-1}$. (The catalyst had been heated to 800°C for 10 h.) Thus, even at the higher loadings, the coverage of the MgO by BaO may not be complete. For the catalysts used in the study described here, about 2.5 mol% BaO corresponds to the theoretical monolayer coverage, assuming that MgO has a surface area of 38 $m^2\ g^{-1}$. Based on these results, it appears likely that the 4 and 7 mol% Ba/MgO samples consist of two or more layers of BaO on MgO, with an increasing number of BaO crystallites as the loading increases. Catalytic results for the oxidative coupling of CH_4 show that inhibition by CO_2 is minimal for 1 mol% Ba but is quite significant for 2 mol% Ba, which is taken as evidence that the basicity increases as multilayers of BaO are formed (22). Pure BaO_2 has a melting point of 450°C; therefore, it is not surprising that calcination at 700°C and cooling in air results in a loss of surface area as the Ba loading becomes large (Table 1).

The catalytic properties of Ba/MgO for the direct decomposition of NO are distinctly different for catalysts with barium loadings in the 0.5–7 mol% range when compared to those materials that contain >11 mol% barium, for which the chemistry is dominated by crystalline phases of barium compounds (15, 17). In fact, at the lower loadings, the Ba/MgO catalysts are more similar to the Sr/La_2O_3 catalysts reported by Vannice *et al.* (14) and briefly studied by us (23). For Ba/MgO at lower loadings, the orders of reaction are greater than first-order with respect to NO and negative-order with respect to O_2. Moreover, N_2O is a reaction intermediate. Based on results obtained in our laboratory, the rates of reaction are also comparable to those over Sr/La_2O_3 at 700°C, and the activation energies are nearly the same (23), except for the 7 mol% Ba/MgO catalyst.

There are several mechanisms that result in rate equations which are second order in NO. The one proposed by Vannice *et al.* (18) is a Langmuir–Hinshelwood mechanism in which a quasi-equilibrated NO adsorption step was assumed and a reaction involving adsorbed NO was proposed as the rate determining step:

$$\mathrm{NO\ (g) + s \leftrightarrows NO\text{-}s} \qquad [1]$$

$$\mathrm{2\,NO\text{-}s \rightarrow N_2O\text{-}s + O\text{-}s\ (RDS)} \qquad [2]$$

$$\mathrm{N_2O\text{-}s \rightarrow N_2\ (g) + O\text{-}s} \qquad [3]$$

$$\mathrm{2\,O\text{-}s \rightleftarrows O_2\ (g) + 2\,s.} \qquad [4]$$

If the surface coverage of N_2O is assumed to be small, due to its much weaker adsorption and higher reactivity, as they suggested, the rate equation

$$r = Lk_2K_{\mathrm{NO}}^2P_{\mathrm{NO}}^2\big/\left(1 + K_{\mathrm{NO}}P_{\mathrm{NO}} + K_{\mathrm{O_2}}^{1/2}P_{\mathrm{O_2}}^{1/2}\right)^2 \qquad [5]$$

can be derived, where L represents the total number of surface active sites, k_2 is the rate constant for Reaction [2], and K_{NO} and $K_{\mathrm{O_2}}$ represent adsorption equilibrium constants for NO and O_2, respectively. Their experimental data agree very well with this equation for NO decomposition over La_2O_3 and Sr/La_2O_3 catalysts. In order to check the validity of this mechanism, Eq. [5] was used to fit our experimental data; however, in this case, the N_2 formation rates were obtained in the presence of different amounts of O_2 added to the feed gas and with a fixed NO concentration of 1%. The fitted results obtained with Eq. [5] are shown in Fig. 6, where the symbols and the dashed line represent the experimental data and the fitted results, respectively.

Another Langmuir–Hinshelwood mechanism, which involves the dissociation of adsorbed NO, also gives a rate expression with an NO reaction order of 2. In this mechanism, adsorbed NO molecules dissociate into nitrogen and oxygen atoms, and the surface reaction of adsorbed NO and adsorbed N atoms is proposed as the rate-determining step.

$$\mathrm{NO\ (g) + s \leftrightarrows NO\text{-}s} \qquad [6]$$

$$\mathrm{NO\text{-}s + s \leftrightarrows N\text{-}s + O\text{-}s} \qquad [7]$$

$$\mathrm{NO\text{-}s + N\text{-}s \rightarrow N_2O\text{-}s + O\text{-}s\ (RDS)} \qquad [8]$$

$$\mathrm{N_2O\text{-}s \rightarrow N_2\ (g) + O\text{-}s} \qquad [9]$$

$$\mathrm{2\,O\text{-}s \rightleftarrows O_2\ (g) + 2\,s} \qquad [10]$$

The expression for N_2 formation rate is given by

$$r = Lk_{12}K_{11}K_{\mathrm{NO}}^2P_{\mathrm{NO}}^2K_{\mathrm{O_2}}^{-1/2}P_{\mathrm{O_2}}^{-1/2}\big/ \left(1 + K_{\mathrm{NO}}P_{\mathrm{NO}} + K_{\mathrm{O_2}}^{1/2}P_{\mathrm{O_2}}^{1/2}\right)^2, \qquad [11]$$

in which k_8 represents the rate constant of Reaction [8] and K_7 represents the equilibrium constant for Eq. [7]. The fitted result is shown in Fig. 6 as a dotted line.

An Eley–Rideal mechanism, in which the reaction between the gas-phase NO and a surface reactive species is assumed as the rate-determining step, can give a rate expression which is second order with respect to NO. The proposed mechanism is given as

$$\mathrm{NO\ (g) + s \leftrightarrows NO\text{-}s} \qquad [12]$$

$$\mathrm{NO\ (g) + NO\text{-}s \rightarrow (N_2O_2)\text{-}s\ (RDS)} \qquad [13]$$

$$\mathrm{(N_2O_2)\text{-}s + s \rightarrow N_2O\text{-}s + O\text{-}s} \qquad [14]$$

$$\mathrm{N_2O\text{-}s \rightarrow N_2\ (g) + O\text{-}s} \qquad [15]$$

$$\mathrm{2\,O\text{-}s \rightleftarrows O_2\ (g) + 2\,s.} \qquad [16]$$

In this mechanism, the reaction of a gas-phase NO molecule and adsorbed NO or an N-containing species such as a nitrate or nitrite ion or a dinitrosyl species on the catalyst surface is assumed to be the rate-determining step, and the rate equation derived from this mechanism is

$$r = Lk_{13}K_{\mathrm{NO}}^2P_{\mathrm{NO}}^2\big/\left(1 + K_{\mathrm{NO}}P_{\mathrm{NO}} + K_{\mathrm{O_2}}^{1/2}P_{\mathrm{O_2}}^{1/2}\right), \qquad [17]$$

where k_{13} represents the rate constant of Reaction [13]. The fitted data with rate Eq. [17] is given in Fig. 6 as the solid line. An adsorbed dinitrosyl species has been proposed as the reaction intermediate during NO decomposition over a Cu–ZSM-5 catalyst by Shelef (24). However, by applying first-principles quantum calculations to assess the plausibility of an NO decomposition mechanism, Schneider *et al.* (25) demonstrated that isonitrosyl, rather than dinitrosyl, may act as a reaction intermediate during NO decomposition over Cu–ZSM-5.

For closed-shell oxides (e.g., Ba/MgO and Sr/La_2O_3) that function as catalysts for NO decomposition at high temperatures, it appears more likely that only ionic intermediates, such as NO_2^- or NO_3^-, would have the stability necessary for achieving reasonable surface concentrations. The *in situ* Raman results confirm that these ionic species are indeed formed upon exposure to NO and that they are present at temperatures approaching those employed in the decomposition reaction. If one assumes that nitrite ions may function as a reaction intermediate, the Eley–Rideal mechanism may be modified such that Reactions [12], [13], and [14] are replaced by

$$\mathrm{NO\ (g) + O^-\text{-}s \rightarrow NO_2^-\text{-}s} \qquad [12a]$$

$$\mathrm{NO\ (g) + NO_2^-\text{-}s + s \rightarrow N_2O\text{-}s + O_2^-\text{-}s\ (RDS).} \qquad [13a]$$

The active surface form of oxygen could be regenerated by

$$\mathrm{2\,O_2^-\text{-}s \rightarrow 2\,O^-\text{-}s + O_2\ (g) + \text{-}s.} \qquad [18]$$

Since barium peroxides are known to exist, even at elevated temperatures (26), the reaction

$$\mathrm{O_2^{2-}\text{-}s + s \rightarrow 2\,O^-\text{-}s} \qquad [19]$$

may be important as a source of surface O^- ions. The reaction

$$\mathrm{NO_2^-\text{-}s + 1/2\,O_2\ (g) \rightarrow NO_3^-\text{-}s} \qquad [20]$$

could account for the negative influence of O_2 on the decomposition reaction. Thus, O_2 could have both a positive and a negative effect on the formation of NO_2^- ions; a positive effect through the formation of peroxide ions, followed by Reactions [19] and [12a], and a negative effect through Reaction [20]. The kinetic results obtained at 750°C (Fig. 6) imply that the net effect of O_2 is negative. In the absence of spectroscopic data at the higher temperature, it is not possible to be more certain about the role of nitrite ions in NO decomposition. The influence of O_2 on NO_2^- ion concentration is an alternative to the more conventional view that O_2 decreases the concentration of oxygen vacancies. The latter may be responsible for the small negative effect that O_2 has on N_2O decomposition (Fig. 5). Although N_2O is depicted only as a surface intermediate in all three mechanisms, this species presumably is in a quasi-equilibrium state with gas-phase N_2O.

As shown in Fig. 6, all three models give results that agree with the experimental data reasonably well; therefore, no distinctions can be made on this basis. Other criteria must be considered. It is known that on noble metal catalysts adsorbed NO molecules can dissociate to form adsorbed nitrogen and oxygen atoms; however, it seems unlikely that adsorbed NO molecules can dissociate to N-s and O-s over a metal oxide surface as described in Eq. [7]. For this reason, the second mechanism probably is not applicable for the Ba/MgO catalyst. The first mechanism suffers from the fact that the concentration of molecularly adsorbed NO would be very small at the elevated temperatures of the catalytic process. Thus, the probability of a bimolecular reaction (Reaction [2]) would be small. One could write the mechanism in terms of an ionic NO_2^- species, but, again, the small concentration of these species suggests that this is not a realistic pathway. Obviously, other mechanisms are conceivable, but, of the three, the Eley–Rideal mechanism appears to be the most reasonable.

5. CONCLUSIONS

Barium oxide on MgO, with moderate loadings of Ba, is an active catalyst for NO decomposition at elevated temperatures. The reaction rate increases in a monotonic manner with respect to temperature, in contrast to similar catalysts that contain larger loadings of Ba. Nitrous oxide is formed as a gas-phase intermediate in the NO decomposition reaction, although the N_2 selectivity is large at any reasonable level of conversion because the decomposition rate for N_2O is much larger than that for NO. The kinetics of the reaction (second-order in NO and negative-order in O_2) is consistent with an Eley–Rideal mechanism in which the rate-limiting step involves the reaction of gas-phase NO with an N-containing surface intermediate. Nitrate and nitrite ions are sufficiently stable on the surface to function as intermediates at the elevated reaction temperatures although the particular form of the intermediate remains unclear.

ACKNOWLEDGMENT

This research was supported by the National Science Foundation under Grant CHE-9520806.

REFERENCES

1. Iwamoto, M., Furukawa, H., Mine, Y., Uemura, F., Mikuriya, S., and Kagawa, S., *J. Chem. Soc. Chem. Commun.*, 1272 (1986).
2. Iwamoto, M., and Yahiro, H., *Catal. Today* **22**, 5 (1994).
3. Shelef, M., *Chem. Rev.* **95**, 209 (1995).
4. Chang, Y., and McCarty, J. G., *J. Catal.* **178**, 408 (1998).
5. Hamada, H., Kintaichi, Y., Sasaki, M., and Ito, T., *Chem. Lett.*, 1069 (1990).
6. Shin, S., Hatakeyama, Y., Ogawa, K., and Shimomura, K., *Mater. Res. Bull.* **14**, 133 (1979).
7. Tabata, K., *J. Mater. Sci. Lett.* **7**, 147 (1988).
8. Shimada, H., Miyama, S., and Kuroda, H., *Chem. Lett.*, 1797 (1988).
9. Yasuda, Y., Mizuno, N., and Misono, M., *J. Chem. Soc. Chem., Commun.*, 1094 (1990).
10. Winter, E. R. S., *J. Catal.* **22**, 158 (1971).
11. Zhang, X., Walters, A. B., and Vannice, M. A., *J. Catal.* **146**, 568 (1994).
12. Zhang, X., Walters, A. B., and Vannice, M. A., *Appl. Catal. B Environ.* **4**, 237 (1994).
13. Zhang, X., Walters, A. B., and Vannice, M. A., *J. Catal.* **155**, 290 (1995).
14. Zhang, X., Walters, A. B., and Vannice, M. A., *Appl. Catal. B Environ.* **7**, 321 (1996).
15. Xie, S., Mestl, G., Rosynek, M. P., and Lunsford, J. H., *J. Am. Chem. Soc.* **119**, 10186 (1997).
16. Xie, S., Rosynek, M. P., and Lunsford, J. H., *J. Catal.* **188**, 32 (1999). [Part II of this series]
17. Mestl, G., Rosynek, M. P., and Lunsford, J. H., *J. Phys. Chem. B* **101**, 9321 (1997).
18. Vannice, M. A., Walters, A. B., and Zhang, X., *J. Catal.* **159**, 119 (1996).
19. Amirnazmi, A., Benson, J. E., and Boudart, M., *J. Catal.* **30**, 55 (1973).
20. Vannice, M. A., Walters, A. B., and Zhang, X., *J. Catal.* **159**, 119 (1996).
21. Lunsford, J. H., Yang, X., Haller, K., and Laane, J., *J. Phys. Chem.* **97**, 13810 (1993).
22. Dissanayake, D., Lunsford, J. H., and Rosynek, M. P., *J. Catal.* **143**, 286 (1993).
23. Xie, S., Ballinger, T. H., Rosynek, M. P., and Lunsford, J. H., *Stud. Surf. Catal.* **101**, 711 (1996). [11th Internat. Congr. on Catal., 40th Anniversary]
24. Shelef, M., *Catal. Lett.* **15**, 305 (1992).
25. Schneider, W. F., Hass, K. C., Ramprasad, R., and Adams, J. B., *J. Phys. Chem.* **101**, 4353 (1997).
26. Mestl, G., Rosynek, M. P., and Lunsford, J. H., *J. Phys. Chem. B* **102**, 154 (1998).